$[H_2NMe_2]CuZrCl_6$: Hydrogen-Bond Induced Distortions in a Copper Zirconium Chloride Analogue of a Thiophosphate

Andrew M. Dattelbaum and James D. Martin*

Department of Chemistry, North Carolina State University, Raleigh, North Carolina 27695

Received October 7, 1998

The copper(I) zirconium(IV) halide, $[H_2NMe_2]CuZrCl_6$ (**1**), has been synthesized, and its single-crystal X-ray structure was determined. The crystal undergoes a phase transition at −60 °C giving a room-temperature structure with $a = 10.1105(6)$ Å, $b = 9.9463(5)$ Å, $c = 12.7254(8)$ Å, $\beta = 110.287(5)°$ in the monoclinic space group $C2/c$, $Z = 4$, and a low-temperature structure (−116 °C) with $a = 10.234(2)$ Å, $b = 9.427(1)$ Å, $c = 12.691(2)$ Å, $\beta = 109.90(2)°$ in the monoclinic space group $P2_1/c$, $Z = 4$. $[H_2NMe_2]CuZrCl_6$ is constructed from unique one-dimensional chains with zirconium and copper in alternating octahedral and tetrahedral coordination environments, respectively. The structural relationship between $(CuCl_4)^{3-}$ and $(PS_4)^{3-}$ is demonstrated by the analogy of this structure to that of $KNiPS_4$. The phase transition, which occurs at approximately −60 °C, results in altered configurations of the dimethylammonium to metal−chloride hydrogen bonding. In addition, a remarkable distortion in the cuprous chloride tetrahedral unit is observed in the room-temperature structure, whereas the zirconium chloride octahedron is distorted in the low-temperature crystal structure. These distortions are discussed in terms of hydrogen-bond driven second-order Jahn−Teller-type distortions.

Introduction

Charge-matching techniques have been broadly utilized to specifically tailor the properties of materials within a given structure type. Zeolites represent a classic case where such charge-matching strategies are utilized. For example, the sodalite structure is observed for silicates,[1] aluminosilicates,[2] aluminophosphates,[3] zinc arsnates,[4] etc., all of which can be considered isoelectronic or charge-matched to the parent phase SiO_2. We recently demonstrated an extension of such charge matching techniques to include substitutions of framework anions in the preparation of halozeotypes, $[Cu_nZn_{m-n}Cl_{2m}]^{n-}$, which are direct analogues of aluminosilicates.[5] Our halide-for-oxide substitution strategy, by which novel metal halide materials are designed as charge-matched analogues of metal oxides, can be further utilized to describe $(CuCl_4)^{3-}$ as a charge-matched and isostructural analogue of $(PO_4)^{3-}$ or $(PS_4)^{3-}$. Such phosphate analogues of early transition metals provide an entry into a new class of materials constructed from the tetrahedral, $(CuCl_4)^{3-}$, building blocks and octahedral early transition metal halide building blocks. We report here the synthesis of a Cu(I), Zr(IV) halide material, $[H_2NMe_2]CuZrCl_6$ (**1**), consisting of chains of alternating zirconium octahedra and copper tetrahedra. Such materials prepared from the redox-active copper chloride and Lewis acidic zirconium chloride building blocks are attractive for potential catalytic applications. For example, the catalytic activity of copper(I) chloride in the presence of strong Lewis acids has received attention for the polymerization of olefins[6,7] and the insertion of carbon monoxide into aromatic C−H bonds.[8,9] $AlCl_3$ is commonly employed as the Lewis acid for such catalytic systems, and we recently described the relationship of the copperhaloaluminate framework structures to those of the aluminophosphates.[10] This report describes our initial synthetic preparations of metal halide structural analogues to phosphates using copper chloride and Lewis acidic group IV metals.

Experimental Section

General Procedures. All reactions were performed under an inert atmosphere in a N_2 filled glovebox or using vacuum and Schlenk techniques. CuCl was prepared from Cu metal and $CuCl_2 \cdot 2H_2O$ (Aldrich, 97%) according to a literature procedure.[11] $ZrCl_4$(99.9%) was used as received from Aldrich. Dimethylamine hydrochloride was heated under vacuum at 100 °C for 24 h in order to remove any water from the material. Benzene (Aldrich) was distilled from Na/benzophenone and stored over 4 Å molecular sieves. All powder X-ray diffraction measurements were obtained using an Enraf-Nonius Guinier camera and were indexed with respect to a silicon standard. IR spectra were measured using a Perkin-Elmer 1600 series FT-IR spectrophotometer.

Synthesis of $[H_2NMe_2]CuZrCl_6$ (1). In a thick-walled (12 mm O.D., 8 mm I.D.) fused silica tube were placed 0.099 mg $ZrCl_4$ (0.425 mmol), 0.045 mg of CuCl (0.454 mmol), and 0.035 mg of $[H_2NMe_2]Cl$ (0.429 mmol). On a Schlenk line, 1.0 mL of benzene was added to the reaction vessel. The reaction mixture was frozen in liquid N_2 and sealed with a torch; the fused silica vessel was filled to 25% volume. The reaction mixture was heated to 150 °C for 1 week and then slow-cooled at a rate of 0.05 °C/min to yield a colorless crystalline solid from which a single crystal was isolated for X-ray structure determination. (**Caution!**

(1) Bibby, D. M.; Dale, M. P. *Nature* **1985**, *317*, 157.
(2) (a) Pauling, L. *Z. Kristallogr.* **1930**, *74*, 213. (b) Loens, J.; Schulz, H. *Acta Crystallogr.* **1967**, *23*, 434.
(3) Wilson, S. T.; Lok, B. M.; Mesina, C. A.; Cannon, T. R.; Flanigen, E. M. *J. Am. Chem. Soc.* **1982**, *104*, 1146.
(4) Nenoff, T. N.; Harrison, W. T. A.; Grier, T. E.; Stucky, G. C. *J. Am. Chem. Soc.* **1991**, *113*, 378.
(5) Martin, J. D.; Greenwood, K. B. *Angew. Chem., Int. Ed. Eng.* **1997**, *36*, 2072.
(6) Ziegler, K.; Holzkamp, E.; Breil, H. *Angew. Chem.* **1955**, *67*, 541.
(7) Natta, G. *Macromol. Chem.* **1955**, *16*, 213.
(8) Gatterman, L.; Koch, H. *Chem. Ber.* **1897**, *30*, 1622.
(9) (a) Dilke, M. H.; Eley, D. D. *J. Chem. Soc.* **1949**, 2601. (b) Dilke, M. H.; Eley, D. D. *J. Chem. Soc.* **1949**, 2613.
(10) Martin, J. D.; Leafblad, B. R.; Sullivan, R. M.; Boyle, P. D. *Inorg. Chem.* **1998**, *37*, 1341.
(11) Kaufmann, G. B. *Inorg. Synth.* **1983**, *22*, 101.

10.1021/ic9811906 CCC: $18.00
Published on Web 04/24/1999

When the sealed reaction vessel is heated, significant pressures are generated which can lead to vessel rupture. Appropriate shielding should be utilized, such as placing the reaction vessels in a capped iron pipe during heating.) Guinier X-ray powder diffraction and elemental analysis indicated a single-phase material. This material has also been prepared in single phase from reactions in superheated CH_2Cl_2. Synthesis from a melt of the reagents at 300 °C resulted in a yield of **1** of greater than >95% with <5% of an unidentified impurity, as determined by X-ray powder diffraction. Elem. anal, observed for $C_4H_8NCl_6CuZr$: C, 6.78; H, 2.46; N, 3.77. Calcd C, 5.81; H, 1.95; N, 3.39. IR data (cm^{-1}): 3195 (s), 1624 (m), 1578 (m), 1457 (m), 1393(w), 1013 (m), 871 (w), 811 (m).

X-ray Structure Determination

Room-Temperature Crystal Structure Analysis of 1. A colorless, single crystal of **1** (0.42 × 0.22 × 0.12 mm) was mounted in a Pyrex capillary under a nitrogen atmosphere using silicone grease. Data were collected on an Enraf-Nonius CAD4 diffractometer at 25 °C with monochromatic Mo Kα radiation. Lattice constants were determined by a symmetry-constrained fit of 24 well-centered reflections between $37° < 2\theta < 40°$ and their Friedel pairs. A unique hemisphere, $\pm h$, $\pm k$, l, was collected with 3541 independent reflections measured by $\theta/2\theta$ scans with $0° < 2\theta < 60°$. The data were scaled to three intensity check reflections using a five-point smoothing routine. An empirical absorption correction was applied using ψ scan data.

Systematic absences were consistent with the space group $C2/c$, which was confirmed in the subsequent refinement. All non-hydrogen atoms were found by direct methods using the SIR92 program. The carbon and nitrogen atoms were refined isotropically, and all other non-hydrogen atoms were refined anisotropically. A full-matrix least-squares calculation on 1379 unique reflections [$I > 2.5\sigma(I)$] was used in the final refinement using the NRCVAX programs.[12] Final residuals of $R = 0.028$ and $R_w = 0.040$ were obtained.

Low-Temperature Crystal Structure Analysis of 1. The crystal which was used for the room temperature data collection was removed from the capillary under a flow of argon, placed on the end of a glass fiber, covered in silicone grease, and immediately transferred to the diffractometer where it was cooled to −116 °C under a stream of dry nitrogen. Data were then collected on an Enraf-Nonius CAD4-Mach diffractometer with monochromated Mo Kα radiation. Lattice constants were determined by a symmetry-constrained fit of 24 well-centered reflections between $34° < 2\theta < 38°$ and their Friedel pairs. A unique hemisphere, $\pm h$, $\pm k$, l, was collected with 2010 independent reflections by ω scans with $0° < 2\theta < 50°$. The data were scaled to three intensity check reflections using a five-point smoothing routine. An empirical absorption correction was applied using ψ scan data. Upon cooling, a phase transition took place such that the C-centered reflections ($h + k = 2n + 1$) were observed, indicating the space group $P2_1/c$; this was subsequently confirmed in the final refinement. All of the heavy atoms were located using a Patterson map. The nitrogen, carbon, and hydrogen positions were then found using difference Fourier techniques. All non-hydrogen atoms were refined anisotropically. The hydrogen positions were idealized to N−H = 0.90 Å and C−H = 0.96 Å and then refined isotropically. A full-matrix least-squares calculation on 1407 unique reflections [$I > 2.5\sigma(I)$] was used in the final refinement using the NRCVAX programs.[12] Final residuals of $R = 0.049$ and $R_w = 0.058$ were obtained.

Variable Temperature Studies. After the data collection was complete, the crystal was warmed at 20 °C intervals in order to ascertain the temperature of the phase transition. The unit cell was determined at each temperature from a set of 24 well-centered reflections. In addition, twenty of the defining reflections for the C-centering were measured at each temperature. The grease holding the crystal to the glass fiber softened at −40 °C such that this crystal could not be studied further. A second crystal was mounted on the end of a glass fiber with epoxy, coated in grease, and cooled to −35 °C under a cold stream of dry nitrogen on the diffractometer. Lattice constants were determined, and 20 defining reflections for the C-centering were measured at approximately 5 ± 3 °C intervals, upon cooling from −35 to −65 °C.

Table 1. Parameters Used in EHTB Calculations

atom	χ_i	H_{ii} (eV)	ξ_i	c_1	ξ_i	c_2
Zr	5s	−9.8700	1.81700			
	5p	−6.7600	1.77600			
	4d	−11.1800	3.83500	0.62242	1.50500	0.57822
Cu	4s	−11.4000	2.20000			
	4p	−6.0600	2.20000			
	3d	−14.0000	5.95000	0.59332	2.30000	0.57442
Cl	3s	−26.3000	2.18300			
	3p	−14.2000	1.73300			

Table 2. Calculated Atomic Charges for Chlorides in **1**

room temperature		low temperature	
atom	calcd charge	atom	calcd charge
Cl(1)-long	−0.707	Cl(1)	−0.648
Cl(1)-short	−0.698	Cl(2)	−0.647
Cl(2)	−0.699	Cl(3)	−0.650
		Cl(4)	−0.648
Cl(3)	−0.731	Cl(5)	−0.726
		Cl(6)	−0.718

Table 3. Crystallographic Data for $[N(CH_3)_2H_2]ZrCuCl_6$ (**1**)

formula	$[N(CH_3)_2H_2]ZrCuCl_6$	
formula weight (g/mol)	413.57	
	room temperature	low temperature
temp, °C	25	−116
space group (No.)	$C2/c$ (15)	$P2_1/c$ (14)
a (Å)	10.1105(6)	10.235(2)
b (Å)	9.9463(5)	9.427(1)
c (Å)	12.7254(8)	12.691(2)
β (deg)	110.287(5)	109.90(2)
V (Å^3)	1200.3(1)	1151.3(3)
Z	4	4
ρ_{calcd} (mg cm^{-3})	2.244	2.386
λ(Mo Kα), Å	0.710 73	0.710 73
μ (cm^{-1})	39.3	40.9
R^a	0.028	0.049
$R_w{}^b$	0.040	0.058

$^a R_f = \sum(F_o - F_c)/F_o$. $^b R_w = [\sum(w(F_o - F_c)^2)/wF_o^2)]^{1/2}$.

Extended Hückel Calculations. Extended Hückel[13] tight binding calculations[14] were performed on the $[CuZrCl_6]^-$ 1-D chain using coordinates taken directly from both the room-temperature and low-temperature single-crystal structures and atomic parameters summarized in Table 1. The disorder in the copper position in the room-temperature structure was modeled by utilizing twice the chain repeat unit. Atomic charges given in Table 2 were calculated based on six k points between (0, 0, 0) and (0, 0, $c^*/2$).

Results

A summary of crystallographic data for the room-temperature and low-temperature structure determinations of $[H_2NMe_2]CuZrCl_6$, **1**, is given in Table 3, positional parameters are in Table 4, and selected bond distances are in Table 5. Comparable chains of $[CuZrCl_6]^-$ run along the c direction in both the room-temperature and low-temperature structures. These chains are constructed from alternating zirconium chloride octahedra and copper chloride tetrahedra that share common edges to form a one-dimensional chain, as shown in Figure 1. The opposing edges of the copper chloride tetrahedra require the zirconium chloride octahedra to be linked in an orthogonal pattern along the chain, which is readily visualized by the orientation of the pairs of terminal Zr−Cl bonds on neighboring octahedra. The $[CuZrCl_6]^-$ chain is notably puckered as seen by the Zr−Cu−

(12) Gabe, E. J.; Le Page, Y.; Charland, J.-P.; Lee, F. L.; White, P. S. *J. Appl. Crystallogr.* **1989**, *22*, 384.

(13) Hoffman, R. D. *J. Chem. Phys.* **1963**, *39*, 1397.

(14) Whangbo, M.-H.; Hoffman, R. *J. Am. Chem. Soc.* **1978**, *100*, 6093.

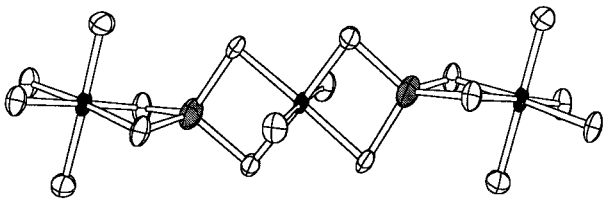

Figure 1. ORTEP drawings of the $[CuZrCl_6]^-$ chains in **1** (low-temperature structure). Thermal displacement ellipsoids are drawn at 95%. Cu atoms are shaded gray, Zr atoms are shaded black, and Cl atoms are unshaded.

Table 4. Atomic Coordinates and Isotropic Displacement Paramters for $[N(CH_3)_2H_2]CuZrCl_6$ (25 and −116 °C)

	x	*y*	*z*	B_{iso}[a]
room temperature				
Zr	0	0	0	2.41(2)
Cu	−0.0080(5)	0.0605(1)	0.2409(4)	5.6(1)
Cl(1)	−0.14980(9)	−0.08332(9)	0.10606(7)	3.67(3)
Cl(2)	0.1032(1)	0.17811(9)	0.14397(6)	3.87(3)
Cl(3)	0.18643(9)	−0.1522(1)	0.10434(8)	4.44(5)
N	0.458(1)	0.120(1)	0.251(2)	10.6(4)
C(1)	0.519(2)	0.052(2)	0.181(1)	8.0(4)
C(2)	0.495(1)	0.052(1)	0.365(1)	6.5(3)
low temperature				
Zr	0.2503(1)	0.2538(1)	0.9996(1)	0.86(3)
Cu	0.2526(1)	0.3043(1)	0.2571(1)	1.63(4)
Cl(1)	0.1097(2)	0.1615(2)	0.1102(1)	1.26(7)
Cl(2)	0.3572(2)	0.4336(2)	0.1518(1)	1.12(7)
Cl(3)	0.4048(2)	0.3393(2)	0.8969(1)	1.23(7)
Cl(4)	0.1466(2)	0.0681(2)	0.8583(1)	1.29(7)
Cl(5)	0.4416(2)	0.0933(2)	0.1045(1)	1.35(7)
Cl(6)	0.0778(2)	0.4233(2)	0.9031(2)	1.46(8)
N	0.3286(6)	0.8023(7)	0.1954(5)	1.6(3)
C(1)	0.2500(9)	0.8129(9)	0.2763(7)	2.1(4)
C(2)	0.2366(8)	0.7821(9)	0.0782(7)	1.9(3)

[a] B_{iso} is the mean of the principal axes of the thermal ellipsoid.

Table 5. Selected Bond Distances (Å) for $[N(CH_3)_2H_2]CuZrCl_6$ (25 and −116 °C)

room temperature		low temperature	
Zr−Cu	3.152(5)	Zr−Cu	3.294(1)
Zr−Cu(b)	3.325(5)	Zr−Cu(b)	3.134(1)
Zr−Cl(1) ×2	2.4939(7)	Zr−Cl(1)	2.485(2)
		Zr−Cl(3)	2.501(2)
Zr−Cl(2) ×2	2.5016(7)	Zr−Cl(2)	2.523(2)
		Zr−Cl(4)	2.471(2)
Zr−Cl(3) ×2	2.4233(8)	Zr−Cl(5)	2.473(2)
		Zr−Cl(6)	2.387(2)
Cu−Cl(1)	2.496(4)	Cu−Cl(1)	2.360(2)
Cu−Cl(2)	2.328(4)	Cu−Cl(2)	2.322(2)
Cu−Cl(1)	2.311(3)	Cu−Cl(3)	2.350(2)
Cu−Cl(2)	2.261(4)	Cu−Cl(4)	2.286(2)
N(a)···Cl(1)	3.45(1), 3.65(1)	N···Cl(2)	3.374(6)
N(a)···Cl(2)	3.41(1)	N···Cl(2)	3.547(6)
N(a)···Cl(3)	3.54(2), 3.85(1)	N···Cl(3)	3.573(7)
		N···Cl(5)	3.333(6)
		N···Cl(5)	3.435(6)

Zr angles of 158.40(5)° and 161.63(4)° for the RT and LT structures, respectively. The Cu−Zr−Cu angles are approximately 180°. The orientation of the alkylammonium cations provides the greatest differentiation between the RT and LT structures (Figure 2); however, significant distortions to the copper chloride and zirconium chloride building blocks are also observed.

Room-Temperature Structure of 1. In the room-temperature structure, the Cu and N atoms are located in the immediate vicinity of 2*m* crystallographic sites. However, an examination

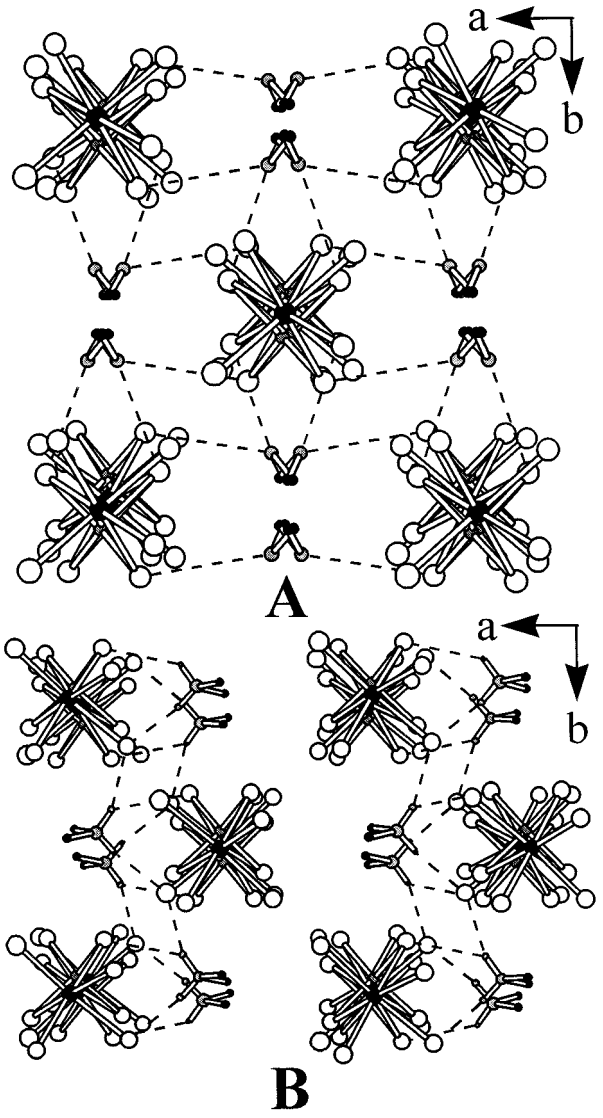

Figure 2. Ball and stick representations of the crystal packing in the room-temperature structure, **A**, and the low-temperature structure, **B**, of **1** viewed down the (001) direction. N···Cl distances <3.5 Å in **A** and NH···Cl distances <2.7 Å in **B** are indicated by dashed lines. Cu and N atoms are shaded gray, Zr and C are black, and Cl atoms are unshaded. The disordered Cu and N(a) positions are both shown in **A**.

of the electron density map revealed multiple maxima at both sites. The electron density map around the nitrogen position revealed five regions of electron density with a clear dominance of two sites, N(a) in Figure 3. The shortest N···Cl contacts for each of the five possible nitrogen positions are also shown in Figure 3, which gives an indication of the possible N−H···Cl hydrogen bonding. Nevertheless, refinement of a simpler two site model with a 50% site occupancy of the dominant N(a) site yielded the most reasonable refinement of both occupancy and isotropic thermal parameters. The disorder of the N positions required a corresponding disorder of the carbon positions in order to achieve a reasonable structural model; this was attempted only for the two-site model of the nitrogen disorder.

The electron density map also clearly indicated that the Cu was disordered across the mirror plane, and thus was refined on a general site with a 50% occupancy. The two positions are symmetrically equivalent and result from the distortion of the copper toward one of two faces within a tetrahedron of four chlorides. Figure 4 illustrates the coordination environment of one of the two symmetrically equivalent copper positions. The

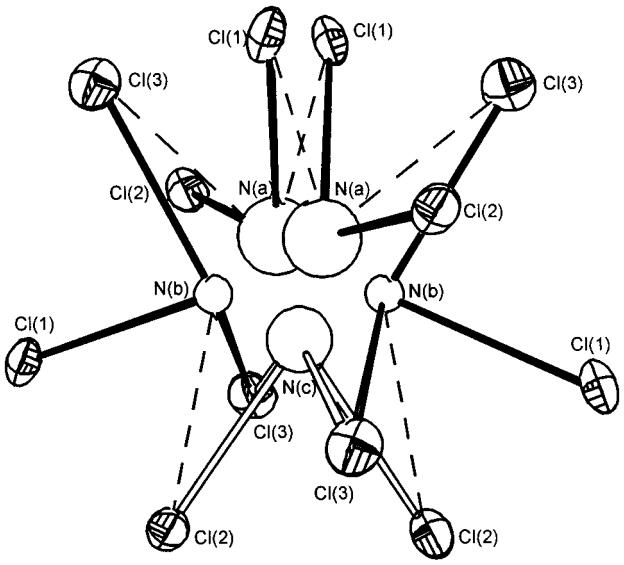

Figure 3. Drawing of the nitrogen positions found in the final difference map of the room-temperature structure are shown along with the closest Cl contacts at each site (N···Cl < 3.49 Å are solid lines, while 3.5 Å < N···Cl < 3.7 Å are dashed lines). The size of the nitrogen atoms have been scaled to the relative electron density at each site.

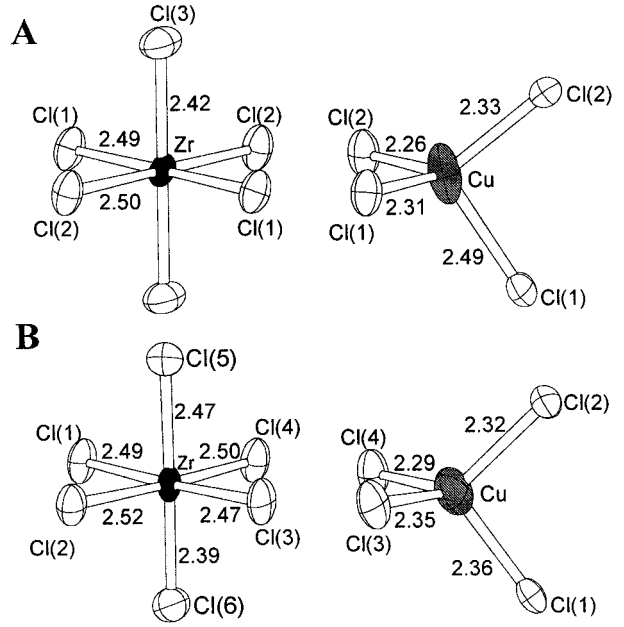

Figure 4. ORTEP drawings showing the distortions of the copper chloride and zirconium chloride building blocks in the room temperature (A) and low temperature (B) structures. Thermal displacement ellipsoids are drawn at 50% for the room-temperature building blocks and 95% for the low-temperature building blocks.

distortion coordinate is along a pseudo-3-fold axis of the tetrahedral building unit and results in the lengthening of one CuCl bond, Cu−Cl(1) = 2.496(4) Å, compared with Cu−Cl(1) = 2.311(3) Å, Cu−Cl(2) = 2.261(4) and 2.328(4) Å. This distortion also results in a flattening of the tetrahedral base with basal Cl_b−Cu−Cl_b angles of 102.3(2)°, 118.38(6)°, and 119.5(2)° and basal/axial Cl_b−Cu−Cl_a angles of 95.1(2)°, 106.79(6)°, and 114.7(2)°. The smallest angles of 102° and 95° correspond to the edges shared with the zirconium octahedra. The thermal displacement ellipsoids for the split copper position are somewhat elongated along the Cu−Cl(1) bond.

In the room-temperature structure, the $ZrCl_6$ octahedra adopt a nearly ideal octahedral geometry with the average Zr−Cl distance of 2.47 Å: Zr−Cl(1) = 2.4939(7) Å, Zr−Cl(2) = 2.5016(7) Å, Zr−Cl(3) = 2.4233(8) Å. The distances to the bridging halides, Cl(1) and Cl(2), are longer than those to the terminal chlorides, as expected. However, the distance of 2.4233(8) Å is relatively long for a terminal Zr−Cl bond when compared to other terminal Zr−Cl bonds (in $ZrCl_4$, Zr−Cl_t = 2.31 Å, and Zr−Cl_b = 2.50 and 2.66 Å).[15]

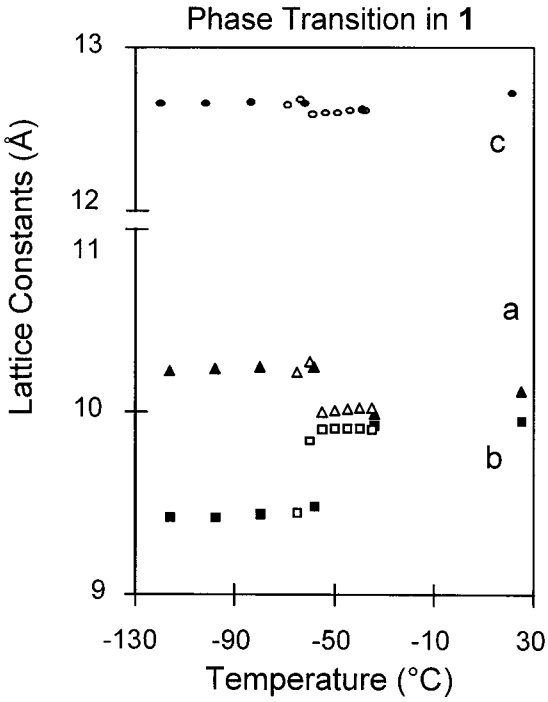

Figure 5. Plot of lattice constants of **1** versus temperature. The *a* lattice constant is plotted as triangles, the *b* lattice constant is plotted as squares and the *c* lattice constant is plotted as ovals. Shaded symbols represent the data for the crystal on warming, and unshaded symbols represent data for a second crystal upon cooling.

Low-Temperature Structure of 1. Diffraction data were collected at −116 °C, and the structure was determined in order to more carefully examine the influence of the hydrogen-bonded ammonium cations on the metal halide chain. A phase transition from a C-centered to a primitive lattice occurred upon cooling the crystal resulting from a reorientation of the ammonium cations as seen in Figure 2. At low temperature, the ammonium cations reside in a site analogous to the N(b) sites of the room-temperature model, alternating the direction of their dipole (protons vs methyl groups) by ±*a*, along the *b* direction. All short N···Cl contacts linking chains along *a* are lost in favor of the formation of interchain hydrogen bonds along *b*. This reorganization from the C-centered cell (RT) to the primitive cell (LT) causes a 0.52 Å contraction of the *b* lattice constant and an expansion of the *a* lattice constant by 0.12 Å as shown in Figure 5. There is no significant change to the *c* lattice constant, which is also the direction of the covalent metal halide chain.

At low temperature, the copper site is fully occupied in approximately the center of a chloride tetrahedron. Nevertheless, a remnant of the room-temperature distortion in the Cu tetrahedron is present but much less obvious in the low-temperature structure, with Cu−Cl bond distances of Cl(1) 2.360(2) Å, Cl(2) 2.322(2) Å, Cl(3) 2.350(2) Å, and Cl(4) 2.286(2) Å. The tetragonal distortion along the shared edges of the chain is the primary distortion from a tetrahedral geometry,

(15) Krebs, B. *Angew. Chem.* **1969**, *81*, 120.

as seen in the bond angles Cl−Cu−Cl = 97.38(7)° and 101.43(7)° for the tetrahedral edges that are shared with the octahedra (vs angles of 109.95(8), 114.31(8), 116.56(8), and 117.31(8)° for the nonshared edges).

By contrast the zirconium chloride octahedron exhibits a striking distortion in the terminal Zr−Cl distances at low temperature. The distances to the four bridging chlorides (Zr(1)−Cl(1) = 2.485(2) Å, Zr(1)−Cl(2) = 2.523(2) Å, Zr(1)−Cl(3) = 2.501(2) Å, and Zr(1)−Cl(4) = 2.471(2) Å) are consistent with expected Zr−chloride bridge distances and the Zr−Cl(6) distance of 2.387(2) Å is consistent with that expected for a terminal chloride.[15] However, the Zr−Cl(5) bond (2.473(2) Å) is elongated by almost 0.1 Å in the direction of the alkylammonium cations.

Phase Transition Temperature. To determine the temperature at which the phase transition occurred, two crystals were examined upon heating (at 20 °C intervals) and cooling (5 °C intervals), respectively, between −116 and −35 °C. An abrupt change in the *a* and *b* lattice constants was observed around −60 °C as shown in Figure 5. The primitive reflections that were systematically extinct in the room-temperature C-centered cell were not observed to grow in upon slow cooling, presumably because of the destruction of crystal quality after passing through the phase transition which resulted in a severe loss in diffraction intensity. When this crystal was warmed back to −35 °C, the high-temperature lattice constants were observed, indicating a reversible phase transition even though the crystal was obviously damaged.

Discussion

A Thiophosphate Analogue. The structural motif exhibited by the chains in **1**, where octahedral building blocks are linked through edge-sharing with tetrahedral units, has been previously observed for $(PPhMe_2)_2Mn_2I_4$[16] and $(DMSO)_2Cd_2I_4$[17] (DMSO = dimethyl sulfoxide). However, to the best of our knowledge **1** is the first homoleptic metal halide material and the first metal chloride to exhibit this structure type. In the manganese and cadmium structures, one metal center is octahedrally coordinated by two terminal, neutral, ligands, and four bridging iodides, while a second metal is tetrahedrally coordinated by four iodides. Such constructions in which a given metal can adopt two distinct coordination geometries is possible due to the d^5 and d^{10} configurations of Mn^{II} and Cd^{II}, respectively, which exhibit no crystal field stabilization.

A more direct structural analogue was identified in the $[MPS_4]^-$ chains (M = Ni[18] or Pd[19]) in which tetrahedral thiophosphate building blocks link square planar metal centers through shared edges. The tetrahedral building block in **1**, $(CuCl_4)^{3-}$, is the charge-matched and structural equivalent of $(PS_4)^{3-}$. Similarly, with two terminal, axial chlorides, $ZrCl_2^{2+}$ is the charge-matched and structural equivalent of the square planar Ni^{2+} or Pd^{2+} building blocks in $(MPS_4)^-$. It is interesting to note, however, that only in the structure of **1** are these octahedral/tetrahedral chains puckered. Except for **1** where the M−M′−M angles are 158.40(5)° at room temperature and 161.63° at low temperature, these analogous chains all exhibit M−M′−M angles of 180°.

Understanding the Metal−Chloride Bond Distortions. Remarkable distortions to the metal chloride bonds are observed in the $CuCl_4$ tetrahedra and $ZrCl_6$ octahedra at room temperature and low temperature, respectively. As described above, in the room-temperature structure, the $CuCl_4$ unit is significantly distorted along the direction of one of the tetrahedral 3-fold axes with the copper moving toward a trigonal planar face resulting in an elongation of one Cu−Cl bond by on the order of 0.2 Å. At room temperature, the zirconium chloride octahedra adopt a nearly ideal geometry in which the terminal Zr−Cl bonds are slightly elongated toward a bond distance nearly equivalent to the bridging chlorides. At low temperature (−116 °C) the distortion pattern is reversed. The distortion from a tetrahedral geometry is minimized for the $CuCl_4$ units, whereas the $ZrCl_6$ octahedra are tetragonally distorted with about a 0.1 Å difference between the two terminal Zr−Cl bonds. The magnitude of these observed distortions is on the order of that expected for Jahn−Teller-type distortions. First-order Jahn−Teller distortions are precluded for the d^{10} tetrahedral and d^0 octahedral fragments. However, in **1**, second-order Jahn−Teller-type distortions, whereby higher lying empty orbitals on the metal and the acceptor orbital of the hydrogen-bond donor mix with the occupied M−Cl σ^* or σ orbitals (schematically represented below), reasonably account for the observed bond distortions. Related second-order distortions have previously been described for other Cu-d^{10} and Zr-d^0 systems.[20,21] In **1** these distortions also appear to be directly related to the formation of hydrogen bonds to the alkylammonium cations.

To understand these distortions, it is necessary to carefully consider the hydrogen bond contacts between the alkylammonium cations and the metal halide chains. Crystal packing requirements with respect to the orientation of the dimethylammonium cations in the structure of **1** appear to be quite flexible, as seen by the difference between the ambient and low-temperature structural solutions, and the possible disordered sites of the ammonium cations in the room-temperature structure. Curiously, though, in the room-temperature structure, the preferred orientation is such that the closest hydrogen-bonding contacts are between the ammonium cations and the bridging chlorides, which are expected to carry a smaller negative charge than the terminal chlorides. A one-dimensional extended Hückel band structure calculation of this chain confirms that the terminal halides have a higher charge density (−0.731) than do the bridging halides (−0.698 and −0.707). Nevertheless, N···Cl contacts of 3.45(1) and 3.65(1) Å to bridging Cl(1) and 3.41(1) Å (*and 4.21(1) Å*) to bridging Cl(2) are observed whereas somewhat longer contacts to the terminal Cl(3), 3.54(2) and 3.85(1) Å, are observed. (The two distances given correspond to the distances to each of the two disordered nitrogen sites.) Although the description of the hydrogen bonding is complicated by disorder of the ammonium cation, the average contacts, 2 × 3.55 Å to Cl(1), 2 × 3.81 Å to Cl(2), and 2 × 3.69 Å to Cl(3) suggests that the hydrogen bonding to Cl(1) > Cl(3) > Cl(2). This precisely corresponds with the direction of the dramatic Cu−Cl(1) bond elongation in the room-temperature structure. Interestingly, each of the two lesser occupied nitrogen sites exhibit shorter contacts to the terminal halide (N(b)···Cl(3) = 3.61 and 3.66 Å and N(c)···Cl(3) = 3.29 Å). By contrast, at low temperature no disorder in the structure is observed and

(16) Beagley, B.; Briggs, J. C.; Hosseiny, A.; Hill, W. E.; King, T. J.; McAuliffe, C. A.; Minten, K. *J. Chem Soc., Chem. Commun.* **1984**, 305.
(17) Nieuwenhuyzen, M.; Wen, H.; Wilkens, C. J. *Z. anorg. Allg. Chem.* **1992**, *615*, 143.
(18) Elder, S. H.; Van der Lee, A.; Brec, R.; Canadell, E. *J. Solid State Chem.* **1995**, *116*, 107.
(19) Chondoudis, K.; Kanatzidis, G.; Sayettat, J.; Jobic, S.; Brec, R. *Inorg. Chem.* **1997**, *36*, 5859.
(20) Burdett, J. K.; Eisenstein, O. *Inorg. Chem.* **1992**, *31*, 1758.
(21) Kang, S. K.; Albright, T. A.; Eisenstein, O. *Inorg. Chem.* **1989**, *28*, 1613.

Scheme 1

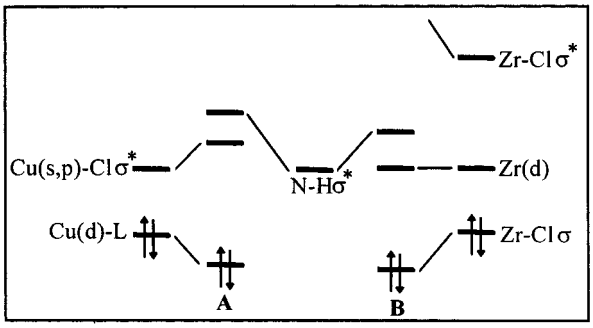

the orientation of the dimethylammonium cations is consistent with the expected strongest hydrogen bond formation to the terminal chloride, NH···Cl(5) = 2.60 and 2.63 Å (N···Cl(5) = 3.33 and 3.43 Å), whereas longer contacts are observed to the bridging chlorides, NH···Cl(2) = 2.63 and 3.17 Å (N···Cl(2) = 3.37 and 3.55 Å) and NH···Cl(3) = 3.06 Å (N···Cl(3) = 3.57 Å). This, too, corresponds precisely to the distortion of the Zr−Cl(5) bond at low temperature.

Distortion of the $CuCl_4$ Tetrahedra. In their recent discussion of the complex coordination chemistry of copper(I) and silver(I) with relation to occurrence of ionic conduction, Burdett and Eisenstein noted that the relatively low energy of the unoccupied Cu (s, p) orbitals allows for significant mixing with occupied Cu 3d orbitals.[20] Because these orbitals are Cu−Cl antibonding in character, mixing with the occupied 3d orbitals results in structural distortions of which the most favored appears to be movement of the metal toward one trigonal plane of ligands. They further noted that such distortions are not observed for systems with large energetic separation between the 3d and the 4s and 4p orbitals, such as is the case for zinc(II). We suggest, as shown in Scheme 1A, that overlap with the unoccupied acceptor orbital of the alkylammonium hydrogen-bond donor can further stabilize the Cu (s, p) orbital and thus reduce the promotional energy required for this second order mixing. Since the charge on the terminal chloride is greater than that of the elongated bridging chloride in the room-temperature model, it is reasonable to suggest that the structural reorganization results from the stabilization brought about by the second-order mixing rather than only a redistribution of charge. Why then is there a difference between the room- and low-temperature structures? At low temperature the ammonium cations are locked into an orientation which prevents significant mixing with the copper chloride tetrahedra. A reorganizational energy for the alkylammonium cation, which must be on the order of kT, must be overcome in order to bring the hydrogen-bond donor into a geometry appropriate to induce the second-order orbital mixing.

Distortion of the $ZrCl_6$ Octahedra. At low temperature, the ammonium cations are frozen into the geometry that maximizes the interaction between hydrogen-bond donor and the more highly charged terminal chlorides of the hydrogen-bond acceptor. While this orientational preference appears to be dominated by the electrostatic attraction between donor and acceptor, the corresponding elongation of Zr−Cl(5) by 0.1 Å with respect to Zr−Cl(6) appears also to result from a second-order mixing of the occupied Zr−Cl bonding orbitals with the acceptor orbitals of the hydrogen-bond donor, as shown in Scheme 1B. Related distortions derived from orbital-mixing have been described by Kang, Eisenstein, and Albright for other d^0 systems such as the trigonal prismatic distortion of $ZrMe_6^{2-}$ in which a second-order Jahn−Teller distortion mixes the unoccupied metal-based orbitals into the occupied M−X bonding orbitals.[21] The symmetry of the extended chain of **1** precludes significant mixing of the Zr d orbitals, however, a mixing of the low-lying and empty ammonium acceptor orbital and high lying Zr p orbitals with the occupied Zr−Cl bonds results in the observed tetragonal distortion. Interestingly, only a much smaller elongation of the Zr−Cl(2) bond is observed in the low-temperature structure of **1** where N···Cl distances reasonable for hydrogen bonds are present but the orientation of the NH bonds are not favorable, thus indicating the directional requirements of the orbital overlap induced distortion. While of smaller magnitude, hydrogen bonding of the ammonium cations to the terminal Zr−Cl(3) bonds in the room-temperature structure also accounts for its elongation to a distance similar to that of a bridging Zr−Cl bond.

The distortions observed in the copper chloride and zirconium chloride bonds of **1** are thus consistent with a significant charge transfer component, as opposed to a solely electrostatic model, of hydrogen bonding. On the basis of this structural chemistry we suggest that the orbital mixing arguments account for the magnitude and directionality of the observed metal chloride bond distortions, but that electrostatic components likely account for a majority of the strength of hydrogen bonds.

Acknowledgment. We thank Ann E. Bunner for the contributions she made on this project as part of a summer high school research program and Dr. Paul Boyle for collecting the crystallographic data. This work was supported by the National Science Foundation CAREER Award (DMR-9501370) and instrumentation grant (CHE-9509532). J.D.M. is a Cottrell Scholar of the Research Corporation.

Supporting Information Available: X-ray crystallographic files, in CIF format, are available for both the room and low-temperature structures of **1** free of charge via the Internet at http://pubs.acs.org.

IC9811906